

Thermal relaxation processes probed by intersubband and inter-valence-band transitions in $\text{Si}/\text{Si}_{1-x}\text{Ge}_x$ multiple quantum wells

B. Adoram, D. Krapf, J. Shappir, and A. Sa'ar

Department of Applied Physics, The Fredi and Nadine Herrmann School of Applied Science, The Hebrew University of Jerusalem, Jerusalem 91904, Israel

M. Levy and R. Beserman

Solid State Institute and Physics Department, The Technion, Haifa 32000, Israel

S. G. Thomas and K. L. Wang

Department of Electrical Engineering, 66-147B Engineering IV, University of California at Los Angeles, California 90095

(Received 7 July 1999; accepted for publication 4 August 1999)

Thermal relaxation processes due to strain relaxation and Si/Ge interdiffusion were investigated in pseudomorphic *p*-type SiGe/Si quantum wells using infrared-polarization-resolved absorption spectroscopy. The samples were annealed from room temperature up to 1060 °C and intersubband transitions between the lowest heavy-hole states and inter-valence-band transitions between heavy-hole and spin-split-off hole states were utilized to probe thermal activation processes. The strain relaxation process is activated at temperatures above 750 °C and causes a decrease of the intersubband absorption and an increase of the inter-valence-band absorption. At temperatures above 940 °C, we found that a second process of Si/Ge interdiffusion causes a reduction of all absorption lines in the spectrum. We proposed a simple model that provides a qualitative explanation to the above results. © 1999 American Institute of Physics. [S0003-6951(99)00641-5]

Heterostructures based on silicon (Si) and silicon-germanium (SiGe) alloys have attracted considerable interest in recent years, mainly due to continued progress in epitaxial growth technology and the ability to fabricate devices compatible with silicon based integrated-circuit technology. Examples of such devices are SiGe heterostructure bipolar transistors (HBTs),¹ SiGe metal-oxide-semiconductor (MOS) transistors,² and SiGe photodiodes.³ Other remarkable examples are the SiGe quantum well infrared photodetectors (QWIPs).⁴⁻⁷ SiGe QWIPs offer an alternative to GaAs based QWIPs⁸ with the advantage of being compatible with standard Si technology. Pseudomorphic *p*-type Si/SiGe quantum wells (QWs) exhibit optical transitions within the valence band at mid-infrared wavelengths⁹⁻¹¹ and detectors based on these transitions were demonstrated.⁴⁻⁷ However, so far the reported performances of SiGe QWIPs are somewhat inferior to that of *n*-type and *p*-type GaAs QWIPs. One reason for that is associated with the difficulty in utilizing the advantages of the advanced silicon processing technology during the fabrication of SiGe QWIPs. For example, oxidation and diffusion during the fabrication process require thermal treatment at high temperatures.¹² It is, therefore, essential to understand the influence of thermal annealing processes on the optical properties of pseudomorphic *p*-type SiGe QWs.

In this letter we present a systematic experimental study of the optical properties associated with transitions within the valence band of a SiGe multiple QW structure under thermal treatments. The sample used for our experiments was grown by molecular beam epitaxy (MBE) on a high resistivity (1500 Ω cm) *n*-type (100) Si substrate. The structure consists of 20 periods of SiGe/Si QWs. Each period consists of a 30-Å wide $\text{Si}_{0.77}\text{Ge}_{0.23}$ QW, boron (*p*-type) doped to a level of $9.6 \times 10^{11} \text{ cm}^{-2}$, and a 500 Å undoped Si barrier. In addition, a 300-Å-wide $\text{Si}_{0.77}\text{Ge}_{0.23}$ layer, *p*-type

doped to a level of $4 \times 10^{18} \text{ cm}^{-3}$, was grown on top of the QWs. The whole structure is capped with 5000 Å top and bottom Si layers.

Infrared absorption measurements were performed using a Perkin-Elmer 2000 Fourier transform infrared (FTIR) spectrometer at room temperature. The samples were prepared in the commonly used multi-path waveguide geometry with the two edge facets polished in 45°. A built-in polarizer (inside the FTIR) was used to rotate the polarization of the incident infrared beam from 0° [transverse magnetic (TM) polarization perpendicular to the growth direction] to 90° [transverse electric (TE) polarization parallel to the growth direction].

Infrared transmission spectra at various polarization angles of the as grown sample are shown in Fig. 1. Absorption peaks at 10.0, 6.1, and at 3.8 μm were observed. Figure 1(a) shows a strong TM absorption line at 10.0 μm that is polarized along the growth direction. We assign this transition to the HH1→HH2 intersubband transition (ISBT) in the QWs (where HH stands for heavy-hole states).^{4,5,10} In Fig. 1(b) we show two additional TE absorption lines that are polarized perpendicular to the growth direction and are assigned to inter-valence-band transitions (IVBTs) in the QW (3.8 μm) and in the 300-Å-wide SiGe layer (6.1 μm).^{6,9-11} The IVBT energy at 6.1 μm fits very well to the energy separation of the HH→SO in semibulk strained $\text{Si}_{0.77}\text{Ge}_{0.23}$ (where SO stands for spin-split-off hole states). The second transition is assigned to HH1→(SO+LH)1 IVBT in the QWs (since non-negligible mixing between SO and light-hole (LH) states takes place in QWs,¹⁰ we denote this state by SO+LH).

Next, the samples were annealed in a furnace for 1 h at temperatures between room temperature and 1060 °C under nitrogen gas ambient and the infrared spectra were recorded after each thermal process. The insets of Figs. 2(a) and 3(b)

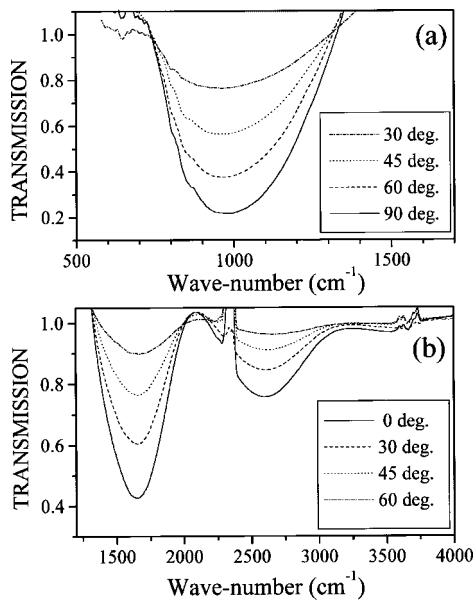


FIG. 1. Transmission spectra of *p*-type Si/SiGe OWs at various polarization angles. (a) Transmission spectra normalized to 0° (i.e., TE polarization) showing the HH1→HH2 ISBT (b) Transmission spectra normalized to 90° (TM) of IVBTs. The lines at 2300 and 3600–3700 cm⁻¹ are related to atmospheric absorption.

show the absorption spectra after various annealing temperatures where only the most polarized spectrum is shown for each temperature and absorption line. The results indicate various thermal processes for each absorption line. To demonstrate that, we show in Fig. 2(a) an Arrhenius plot of the ISBT integrated absorbance (defined as the area below a given absorption line) and the peak energy position of the ISBT absorption versus the annealing temperature [Fig. 2(b)]. Figure 3 shows similar plots for the IVBT transitions.

Two different activation processes can be deduced from these figures. At temperatures higher than 940 °C the integrated absorbance of the QW transitions (ISBT and IVBT) decreases with the increasing temperature. The activation energy for both lines is approximately the same, $\Delta E_G \cong (1.9 \pm 0.2)$ eV. The semibulk IVBT shows a weaker decrease that begins at slightly higher temperatures. In the temperature range, 750–940 °C, we observe a second thermal activation process. Here the QW ISBT integrated absorbance decreases with the increasing temperature with an activation energy of $\Delta E_S \cong (0.13 \pm 0.02)$ eV while the integrated absorbance of both IVBTs increases with increasing temperature with $\Delta E_S \cong (0.09 \pm 0.02)$ eV. In addition, we did not observe a shift of the QW ISBT peak energy while the IVBT lines showed a redshift of the peak energy at temperatures above 800 °C.

The above results can be explained by the following model. The high temperature activation process is assigned to the interdiffusion of Ge/Si atoms between the strained SiGe QWs and the Si barrier regions.^{13,14} This process causes a destruction of the interfaces between the wells and the barriers giving rise to a strong alloy disorder scattering that destroys the coherency of the QW electronic states. The activation energy measured for this process is in reasonable agreement with other reports where Ge/Si interdiffusion in strained layers has been detected by other experimental techniques.^{13,14} Furthermore, to confirm this assumption we

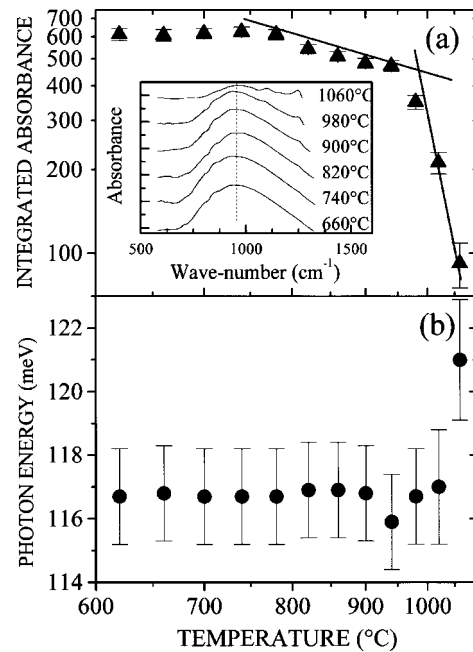


FIG. 2. (a) Arrhenius plot of the ISBT integrated absorbance vs the annealing temperature. The solid lines represent two activation processes. (b) The peak photon energy of the ISBT vs annealing temperature. The inset shows absorption spectra at various annealing temperatures.

conducted a set of Raman spectroscopy experiments on the annealed samples and observed a redshift of the Si–Ge phonon line with increasing annealing temperature as expected for an interdiffusion process.^{14,15} The semibulk IVBT is expected to be less sensitive to this process since interdiffusion should destroy the entire SiGe region rather than the interfaces.

The mid-temperature activation process is assigned to thermally activated strain relaxation in the pseudomorphic SiGe layers.^{15–18} Here again, a blueshift of the strained Si–Si and a redshift of the Si–Ge phonon lines, obtained from Raman spectroscopy, provide support to this assertion.¹⁵ It is well known that in-plane biaxial strain in SiGe layers causes a removal of the degeneracy between the heavy- and light-

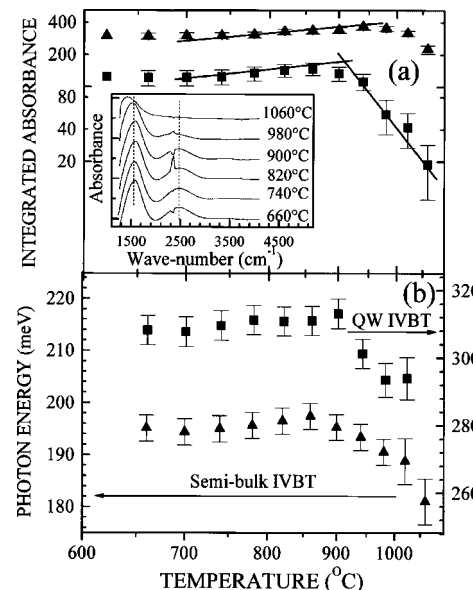


FIG. 3. The same as Fig. 2 for the IVBTs [QW (▲) and semibulk (■) transitions].

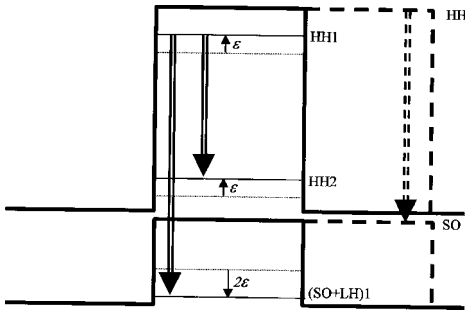


FIG. 4. Schematic illustration showing the effect of the strain on the valence-band structure and the optical transitions. The strain causes both heavy-hole states to be shifted upward while the spin-split-off state is shifted downward. Also shown are the QW transitions (solid lines) and the semi-bulk IVBT transition in the wider well (dashed line).

hole valence bands at the Γ point and a mixing of the light-hole and the spin-split-off bands.¹⁹ A simple model to explain the effect of strain relaxation on the valence band can be obtained by writing the valence band Hamiltonian as $H(\epsilon) = H_0 + \Delta H(\epsilon)$, where H_0 is the valence band Hamiltonian in the absence of strain (that can be described, for example, by the Luttinger–Kohn model²⁰) and $\Delta H(\epsilon)$, the contribution of the strain, can be approximated as follows:

$$\Delta H(\epsilon) = \begin{bmatrix} \epsilon & 0 & 0 \\ 0 & -\epsilon & -i\sqrt{2}\epsilon \\ 0 & i\sqrt{2}\epsilon & 0 \end{bmatrix}, \quad (1)$$

where ϵ is the strain energy. Diagonalization of $\Delta H(\epsilon)$ yields: $E_{HH} \rightarrow E_{HH} + \epsilon$, $E_{LH} \rightarrow E_{LH} + \epsilon$, and $E_{SO} \rightarrow E_{SO} - 2\epsilon$. Although the above results hold for an infinite QW only, they provide a qualitative explanation to the experimental observations as schematically illustrated in Fig. 4. The $HH1 \rightarrow (SO+LH)1$ transition is redshifted by $3\Delta\epsilon$ during strain relaxation (where $\Delta\epsilon$ is the amount of thermal strain energy relaxation). However, the $HH1 \rightarrow HH2$ transition is not shifted by strain relaxation in the case of infinite QW since both states are displaced by the same amount. Notice that in a finite QW one may find a weak dependence of the ISBT on the strain energy, but this weak effect is expected to be screened by the relatively large linewidth of the transition. Similar redshift is expected for the semi-bulk $HH \rightarrow SO$ transition.

The above model can also provide a qualitative explanation to the various activations of the integrated absorbance during the annealing. The integrated absorbance (IA) is proportional to $IA_{ISBT} \propto |\langle HH1 | p_z | HH2 \rangle|^2$ and $IA_{IVBT} \propto |\langle HH1 | \mathbf{p}_\perp | (SO+LH)1 \rangle|^2$ where p_z and \mathbf{p}_\perp are components of the momentum operator along and perpendicular to the growth direction of the ISBT and IVBT, respectively. With decreasing strain energy, the $HH2$ envelope state is pushed down toward the edge of the QW and becomes less and less localized in the well. As a result, the integrated absorbance of the $HH1 \rightarrow HH2$ ISBT decreases with increasing annealing temperature. On the other hand, the IVBT transition dipole is composed of a Bloch states dipole matrix element, that to a first order approximation is not affected by the strain, times the overlap between the envelope states. Hence, from Eq. (1) we see that the most significant effect of the strain is the mixing between the localized $SO1$ envelope state and the

delocalized $LH1$ envelope state (the energy level of this state is above the LH barrier). As a result, strain relaxation causes decoupling of the $SO1$ state (and the SO state of the bulk) from the delocalized LH component of the entire envelope wave function giving rise to a larger overlap of the $HH1 \rightarrow (SO+LH)1$ transition.

The strain relaxation process in $SiGe/Si$ was found to be enhanced in the temperature range $700\text{--}800^\circ\text{C}$ ¹⁶ and is in agreement with our results. Furthermore, following Ref. 19 the energy difference between fully strained and relaxed $Si_{0.77}Ge_{0.23}$ is about $\Delta E_S \cong 0.1$ eV. This energy should be on the order of the activation energy for local strain relaxation, in reasonable agreement with our findings. Notice also that similar activation energies were measured by other experimental techniques.^{15,18}

In conclusion, we found that two activation processes take place during annealing of pseudomorphic $SiGe/Si$ QWs. The first process is strain relaxation that is activated at temperatures above 750°C . This process causes a decrease in the QW ISBT absorption and an increase in the IVBT absorption lines. The second high temperature activation process is related to Ge/Si interdiffusion that results in a decrease of all types of optical transitions in the valence band.

This work was partially supported by Grant No. 5877 of the Israeli Ministry of Science.

- ¹F. Schaffler, D. Tobben, H.-J. Herzog, G. Abstreiter, and B. Hollander, *Semicond. Sci. Technol.* **7**, 260 (1992).
- ²P. M. Garone, V. Venkataraman, and J. C. Sturm, *IEEE Electron Device Lett.* **13**, 56 (1992).
- ³B.-Y. Tsaur, C. K. Chen, and S. A. Marino, *IEEE Electron Device Lett.* **12**, 293 (1991).
- ⁴R. P. G. Karunasiri, J. S. Park, and K. L. Wang, *Appl. Phys. Lett.* **59**, 2588 (1991).
- ⁵R. P. G. Karunasiri, J. S. Park, and K. L. Wang, *Appl. Phys. Lett.* **61**, 2434 (1992).
- ⁶R. People, J. C. Bean, C. G. Bethea, S. K. Spitz, and L. J. Peticolas, *Appl. Phys. Lett.* **61**, 1122 (1992).
- ⁷P. Kruck, M. Helm, T. Fromherz, G. Bauer, J. F. Nutzel, and G. Abstreiter, *Appl. Phys. Lett.* **69**, 3372 (1996).
- ⁸B. F. Levine, *J. Appl. Phys.* **74**, R1 (1993).
- ⁹K. L. Wang and R. P. G. Karunasiri, in *Semiconductor Quantum Wells and Superlattices for Long-Wavelength Infrared Detectors*, edited by M. O. Manasreh (Artech House, Boston, 1993), pp. 139–205; J. S. Park, R. P. G. Karunasiri, and K. L. Wang, *Appl. Phys. Lett.* **61**, 681 (1992).
- ¹⁰T. Fromherz, E. Koppensteiner, M. Helm, G. Bauer, J. F. Nutzel, and G. Abstreiter, *Phys. Rev. B* **50**, 15073 (1994); T. Fromherz, P. Kruck, M. Helm, G. Bauer, J. F. Nutzel, and G. Abstreiter, *Appl. Phys. Lett.* **68**, 3611 (1997).
- ¹¹S. Zanier, J. M. Berroir, Y. Guldner, J. P. Vieren, I. Sagnes, F. Glowacki, Y. Campidelli, and P. A. Badoz, *Phys. Rev. B* **51**, 14311 (1995).
- ¹²*ULSI Technology*, edited by C. Y. Chang and S. M. Sze (McGraw–Hill, New York, 1996).
- ¹³T. Walther, C. J. Humphreys, A. G. Cullis, and D. J. Robbins, *Inst. Phys. Conf. Ser. No. 157* (IOP, Bristol, 1997), pp. 47–54, and references therein.
- ¹⁴K. Dettmer, W. Freiman, M. Levy, Yu. L. Khait, and R. Beserman, *Appl. Phys. Lett.* **66**, 2376 (1995).
- ¹⁵R. Rodrigues, T. Rodrigues, A. Kling, J. C. Soares, M. F. Da Silva, and C. Ballesteros, *J. Electron. Mater.* **28**, 77 (1999).
- ¹⁶M. R. Sardela and G. V. Hansson, *J. Vac. Sci. Technol. A* **13**, 314 (1995).
- ¹⁷D. J. Lockwood and J.-M. Baribeau, *Phys. Rev. B* **45**, 8565 (1992).
- ¹⁸J.-P. Noel, N. L. Rowell, D. C. Houghton, and D. D. Perovic, *Appl. Phys. Lett.* **57**, 1037 (1990).
- ¹⁹R. People, *Phys. Rev. B* **32**, 1405 (1985).
- ²⁰G. Bastard, *Wave Mechanics Applied to Semiconductor Heterostructures* (Les Editions de Physique, Les Ulis, 1988).